Theoretical Determination of Activation Free Energies for Alkaline Hydrolysis of Cyclic and Acyclic Phosphodiesters in Aqueous Solution

Xi Chen and Chang-Guo Zhan*

College of Chemistry, Central China Normal University, Wuhan 430079, P. R. China and Department of Pharmaceutical Sciences, College of Pharmacy, University of Kentucky, 907 Rose Street, Lexington, Kentucky 40536

Received: January 6, 2004; In Final Form: March 7, 2004

First-principles electronic structure calculations were performed in this study to examine the reaction pathway and corresponding activation free energies for alkaline hydrolysis of representative phosphodiesters, including dimethyl phosphate (DMP), trimethylene phosphate (TMP), ethylene phosphate (EP), and a simplified model (cAMPm) of adenosine 3′, 5′-phosphate (cAMP). Reaction coordinate calculations show that for all of these phosphodiesters the alkaline hydrolysis follows a one-step bimolecular mechanism initialized by the attack of hydroxide ion at the phosphorus atom of the ester. Five self-consistent reaction field (SCRF) methods were used to calculate the activation free energies and the calculated results were compared with available experimental data. It has been shown that the results calculated using a recently developed SCRF method, known as the surface and volume polarization for electrostatics (SVPE) or fully polarizable continuum model (FPCM), which accurately determines both surface and volume polarization, are rather insensitive to the used solute charge isodensity contour value that determines the solute cavity size. The SVPE calculations plus nonelectrostatic interaction corrections led to activation free energies 32.6, 31.6, 24.8, and 29.4 kcal/mol for DMP, TMP, EP, and cAMPm, respectively. The calculated activation free energies are all in good agreement with available experimentally estimated activation free energies ∼32, ∼32, ∼21−24, and ∼29 kcal/mol for DMP, TMP, EP, and cAMP, respectively. The SVPE results show that the solvation dramatically decreases the activation free energies for the alkaline hydrolysis of phosphodiesters and strongly support the conclusion that the remarkable difference in the hydrolysis rate between DMP and EP is mainly due to the solvation, rather than the ring-strain. Compared to the SVPE results and available experimental data, an SCRF method that completely ignores volume polarization systematically overestimated the activation free energies, but the relative values of the calculated activation free energies are still in qualitative agreement with those of the SVPE results and available experimental data. The other three SCRF methods using a certain charge renormalization scheme also overestimated the activation free energies, and the relative values of the calculated activation free energies are all significantly different from those of the SVPE results and available experimental data.

Introduction

The hydrolysis of phosphate esters is one of the most fundamental chemical and biochemical reactions.[1] Of various phosphate esters, phosphodiesters are particularly interesting. For example, both the biopolymers DNA and RNA consist of phosphodiesters; each monomer is a phosphodiester and dimethyl phosphate (DMP) may be regarded as the simplest model of a DNA molecule in terms of the ester hydrolysis. The intracellular second messenger 3′, 5′-adenosine phosphate (cAMP) is essential in vision, muscle contraction, neurotransmission, exocytosis, and differentiation.[2] Trimethylene phosphate (TMP) has the same six-membered ring as cAMP and can be regarded as a simplified model of cAMP. Ethylene phosphate (EP), known for its unusual ester hydrolysis rate in neutral aqueous solution,[3] is a representative of five-membered cyclic phosphodiesters and has received great attention.

Concerning reaction pathways for the hydrolysis of phosphate esters in aqueous solution, it has been considered that the hydrolysis of the monoesters proceeds by a dissociative, unimolecular elimination pathway, whereas the hydrolysis of the diesters and triesters follow a bimolecular base-catalyzed hydrolysis mechanism.[4,5,6] The bimolecular base-catalyzed hydrolysis is initialized by the nucleophilic attack of a hydroxide ion at the phosphorus atom of the ester. However, Florian and co-workers[7,8] recently questioned a long-standing mechanistic postulate for the phosphate monoester hydrolysis mechanism. They reexamined the available experimental data and found that although the experimental results for reactions in aqueous solution had usually been considered as the evidence for the dissociative pathway, a closer thermodynamic analysis of observed linear free energy relationships showed that the experimental information is consistent with the associative, concerted, and dissociative alternatives.[8] So, it is currently not clear which reaction pathway dominates the hydrolysis of the monoesters. Their work clearly illustrates that reliable computational studies of fundamental reaction pathways and the corresponding energetics are necessary even for chemical reactions in solution that have been thoroughly investigated by experiments.

Theoretical studies on the hydrolysis mechanism of phosphotriester paraoxon and the structural variants[9] reveal that in

* To whom all correspondence should be sent. E-mail: zhan@uky.edu.

10.1021/jp049938v CCC: $27.50
Published on Web 07/03/2004

the nucleophilic reaction the hydroxide ion is positioned near the extension line of the departing oxygen atom and the phosphorus center. The calculated results also indicate that the hydroxide ion-catalyzed hydrolysis involves a pentacoordinated phosphorus intermediate for all examined compounds, except paraoxon. For paraoxon, the expected pentacoordinated phosphorus intermediate does not exist and the hydroxide ion-catalyzed hydrolysis is a single-step process as an S_N2 process.[9] A series of ab initio electronic structure calculations on the base-catalyzed hydrolysis of phosphodiesters and other related phosphate esters reported by Lim and co-workers[10−15] suggest that a dianionic pentacoordinated phosphorus intermediate either does not exist or is only marginally stable, although a singly charged pentacoordinated phosphorus intermediate could exist, during the ester hydrolysis. Dejaegere and co-workers[16,17,18] performed ab initio electronic structure calculations to study the hydroxide ion-catalyzed hydrolysis of a cyclic ethylene phosphate (EP) and an acyclic dimethyl phosphate (DMP) in order to understand the remarkable hydrolysis rate difference between cyclic and acyclic phosphodiesters. It is well-known that the alkaline hydrolysis of EP (a phosphodiester with a five-membered ring) is about 10^6-10^8 times faster than that of DMP (an acyclic phosphodiester), whereas TMP (a phosphodiester with a six-membered ring) reacts at very nearly the same rate as an acyclic phosphodiester.[19] The remarkably higher hydrolysis rate of EP was attributed mainly to the thermodynamic strain of the five-membered ring; the opening of the five-membered ring was thought to be accompanied by release of about 5.5 kcal/mol.[19] Interestingly, Dejaegere and Karplus[16] computationally examined the effects of solvation and ring-strain on the activation free energy for the first step of reaction and concluded that the remarkable difference in hydrolysis rate between cyclic and acyclic phosphodiesters is primarily due to the solvation, rather than the ring-strain.

We note that although Dejaegere and Karplus's[16] results of the calculations on the hydroxide ion-catalyzed hydrolysis of EP and DMP can satisfactorily explain the significant hydrolysis rate difference between these two phosphodiesters, their calculated activation free energy in solution (~38 kcal/mol for DMP) is significantly higher than the corresponding experimental estimate (32 kcal/mol for DMP). The deviation of ~6 kcal/mol tells us that either their electronic structure calculations, particularly the solvation calculations, are not sufficiently accurate or there exists another reaction pathway with a lower activation free energy. Subsequent computational studies[20−24] relevant to the phosphodiester hydrolysis include the further discussion of the ring strain energies, pK_a of phosphoranes representing the possible pentacoordinated phosphorus intermediate structures, and structures and energetics of the transition states calculated with different methods for some individual esters.

We recently performed first-principles electronic structure calculations[25] to study competing reaction pathways and the corresponding activation free energies for ester hydrolysis of two representative cyclic phosphodiesters, that is, TMP and a simplified cAMP model. The reaction coordinate calculations show three fundamental reaction pathways for the ester hydrolysis, including (A) attack of a hydroxide ion at the P atom of the phosphate anion (an S_N2 process without a pentacoordinated phosphorus intermediate), (B) direct attack of a water molecule at the P atom of the anion (a three-step process), and (C) direct attack of a water molecule at the P atom of the neutral ester molecule (a two-step process). The calculated energetic results show that pathway A is dominant for the phosphodiester hydrolysis in neutral aqueous solution. The reliability of our theoretical predictions is supported by the excellent agreement of the calculated activation free energy with available experimental data for the alkaline hydrolysis of TMP in solution.

SCHEME 1: Alkaline Hydrolysis Reactions of Dimethyl Phosphate (DMP), Trimethylene Phosphate (TMP), Ethylene Phosphate (EP), and a Simplified Model (cAMPm) of CAMP

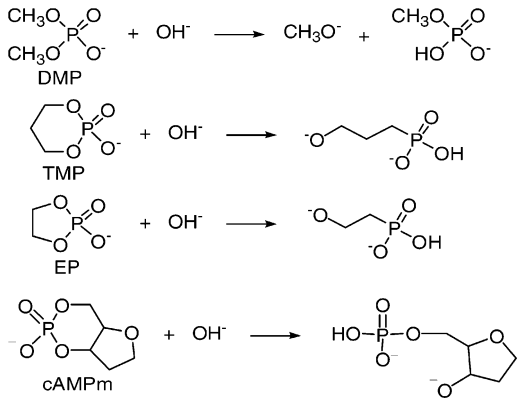

The present study attempts to address two fundamental issues of the phosphodiester hydrolysis. The first is systematic theoretical determination of the activation free energies for the ester hydrolysis of various types of phosphodiesters, including both cyclic and acyclic esters, and for a better understanding of the factors affecting the activation free energies in aqueous solution. The other issue is to know whether first-principles electronic structure calculations with a continuum solvation model can accurately predict the activation free energies or not for alkaline hydrolysis of various phosphodiesters and which continuum solvation model is most suitable for theoretical prediction of these activation free energies. For these purposes, we examined four phosphodiesters, that is, DMP, TMP, EP, and a simplified cAMP model (cAMPm in Scheme 1), as representatives of the acyclic phosphodiesters, cyclic phosphodiesters with a six-membered ring, and cyclic phosphodiesters with a five-membered ring. After geometry optimizations of the transition states and reactants, a variety of self-consistent reaction field (SCRF) methods were performed to evaluate the solvent shifts of the activation free energies. Comparison of the results calculated for different esters can provide useful insights into the factors affecting the activation free energies and comparison of the calculated activation free energies with available experimental data would validate different SCRF calculations.

Calculation Methods. Geometries of all reactants and transition states under consideration in this study were optimized by using the Hartree−Fock (HF) method and the 3-21+G* basis set.[26] The geometries optimized at the HF/3-21+G* level were then refined at the HF/6-31+G* level.[26] Vibrational frequency calculations were carried out to ensure that the optimized geometries are indeed local minima or saddle points on the potential energy surfaces and to determine the zero-point vibration energies and thermal corrections to the Gibbs free energies. Intrinsic reaction coordinate (IRC)[27] calculations were performed at the HF/6-31+G* level to confirm the optimized transition state geometries. The geometries optimized at the HF/6-31+G* level were employed to perform the second-order Møller−Plesset (MP2) energy calculations with the 6-31+G* basis set.

Previous theoretical studies[9,28,29] of reaction pathways for hydroxide ion-catalyzed ester hydrolyses indicate that electron

correlation effects are not important in the optimizations of molecular geometries and calculations of solvent shifts, but are important in final energy calculations, for studying energy profiles of those organic reactions. With a given basis set, the energy barriers evaluated by performing the MP2 energy calculations using the MP2 geometries are all very close to those evaluated by the MP2 calculations using geometries optimized with the HF and density functional theory (DFT) methods. The energy barriers calculated with the MP2 method are all very close to those calculated with the MP4SDQ, QCISD, and QCISD(T) methods,[28] indicating that the MP2 method is sufficiently accurate for recovery of the electron correlation. Regarding the basis set dependence, the energy barriers determined with the 6-31+G* basis set are all very close to those determined with the 6-31++G** and 6-311++G(3d, 3p) basis sets.[9,28] To further examine the accuracy of the energy barriers calculated at the MP2/6-31+G*//HF/6-31+G* level, in the present study additional single-point energy calculations were performed at the MP2/6-31++G**//HF/6-31+G* level for cAMPm.

The geometries optimized at the HF/6-31+G* level in the gas phase were used to perform SCRF energy calculations in aqueous solution in order to determine the solvent shifts. Florian and Warshel[30] performed a manual geometry search in solution along the corresponding gas phase intrinsic reaction coordinate for the hydrolysis of monomethyl phosphate and demonstrated that the contributions of the solvent-induced structural changes to the overall energetics are small and can be safely neglected. Five different SCRF procedures were employed in the solvation calculations on the reactants and transition states to evaluate the activation free energies for the ester hydrolysis in aqueous solution. The first three SCRF procedures employed are the standard polarizable continuum model (PCM),[31] the integral equation formalism for the polarizable continuum model (IEFPCM),[32] and the conductor-like screening solvation model (COSMO)[33] implemented in the Gaussian98[34] program. For these three SCRF procedures, the solute cavity surface is defined as overlapped spheres centered at the solute nuclei, and the contributions of short-range nonelectrostatic interactions, including cavitation, dispersion, and Pauli repulsion, to the energy are also empirically estimated. Besides, these methods use one of four available charge renormalization schemes for the surface polarization charge distribution to formally correct the deviation of the actually calculated total polarization charge from the ideal total polarization charge expected from Gauss Law[35] for the exact solution of Poisson's equation. Obviously, in addition to the employed number of surface nodes (or tesserae) determining the accuracy of the numerical computation, the final results obtained from using these methods depend on many other choices, including the employed radii of the spheres at solute nuclei, the employed charge renormalization scheme, and the employed parameters for the short-range nonelectrostatic interactions. All the PCM, IEFPCM, and COSMO calculations in this study were performed by using the default choices of the Gaussian 98 program for the recommended standard parameters.

The fourth method is known as the surface and volume polarization for electrostatic (SVPE).[36,37,38,39] The SVPE method is also known as the fully polarizable continuum model (FPCM)[40] because it fully accounts for both surface and volume polarization effects in solute−solvent electrostatic interaction. Since the solute cavity surface is defined as a solute charge isodensity contour determined self-consistently during the SVPE iteration process, the SVPE results, converged to the exact solution of Poisson's equation with a given numerical tolerance, depend only on the contour value at a given dielectric constant and a certain quantum mechanical calculation level.[36] By seeking the best overall agreement with experimental conformational free energy differences (62 experimental observations) in various polar solutes existing in various solvents, this single parameter value has been calibrated as 0.001 au.[37] By seeking the best overall agreement with experimental ^{15}N NMR chemical shifts (48 experimental observations) in various polar solutes existing in various solvents, this single parameter value has been calibrated as 0.002 au.[38] However, the 0.001 and 0.002 au contours are all acceptable for the SVPE calculations on both kinds of properties. The final SCRF procedure used determines only the commonly treated surface polarization for the purpose of comparison, and may be called the surface polarization for electrostatic interaction (SPE) model.[36,37,38] Because no charge renormalization scheme was used in the SPE calculations, the differences between the SVPE and SPE results quantitatively represent the effects of volume polarization produced by the solute electron charge distribution outside the solute cavity. SVPE and SPE are both implemented recently into a local version[36]of the GAMESS program.[41] Recent SVPE calculations on hydroxide ion-catalyzed hydrolysis of a series of carboxylic acid esters indicated that the energy barriers determined by the SVPE calculations using both the 0.001 and 0.002 au contours are all qualitatively consistent with the corresponding experimental activation energies.[28,39] The SVPE calculations using the 0.001 au contour slightly and systematically underestimate the energy barriers, whereas the differences between values from the SVPE calculations using the 0.002 au contour and the corresponding average experimental values for the examined esters are smaller than the range of experimental values reported by different laboratories. So, both the 0.002 au contour and the default 0.001 au contour were used in the SVPE and SPE solvation calculations for further comparison in order to examine whether or not such a change to the default 0.001 au contour can significantly change the calculated energy barriers. The dielectric constant of water used for the solvation calculations is 78.5.

Regardless of the difference in the definition of solute cavity size, an advantage of the SVPE method to the PCM, IEFPCM, and COSMO methods is the accurate determination of volume-polarization effects. A disadvantage is that the contribution of short-range nonelectrostatic interaction to solvent shift has not yet been evaluated. It is expected that the contributions of nonelectrostatic interactions to activation free energies, $\Delta G_{\text{non-elec}}$, be largely canceled out during the reaction process. This expectation could be examined quantitatively by evaluating the changes of $\Delta G_{\text{non-elec}}$, determined by PCM, IEFPCM, or the COSMO method. In fact, PCM, IEFPCM, and COSMO implemented in the Gaussian 98 package use the same empirical method to estimate the contributions of nonelectrostatic factors and hence lead to the same $\Delta G_{\text{non-elec}}$ values.

Reaction coordinate calculations in the gas phase and the solvation calculations with PCM, IEFPCM, and COSMO methods were performed by using the Gaussian 98 program.[34] Solvation calculations with SVPE and SPE models were carried out by using a local version[36] of the GAMESS program.[41]

Results and Discussion

The optimized geometries of the four representative phosphodiesters and the corresponding transition states are depicted in Figure 1 along with some key geometrical parameters. As seen in Figure 1, the transition state structures optimized for the four reaction systems are similar to each other in terms of

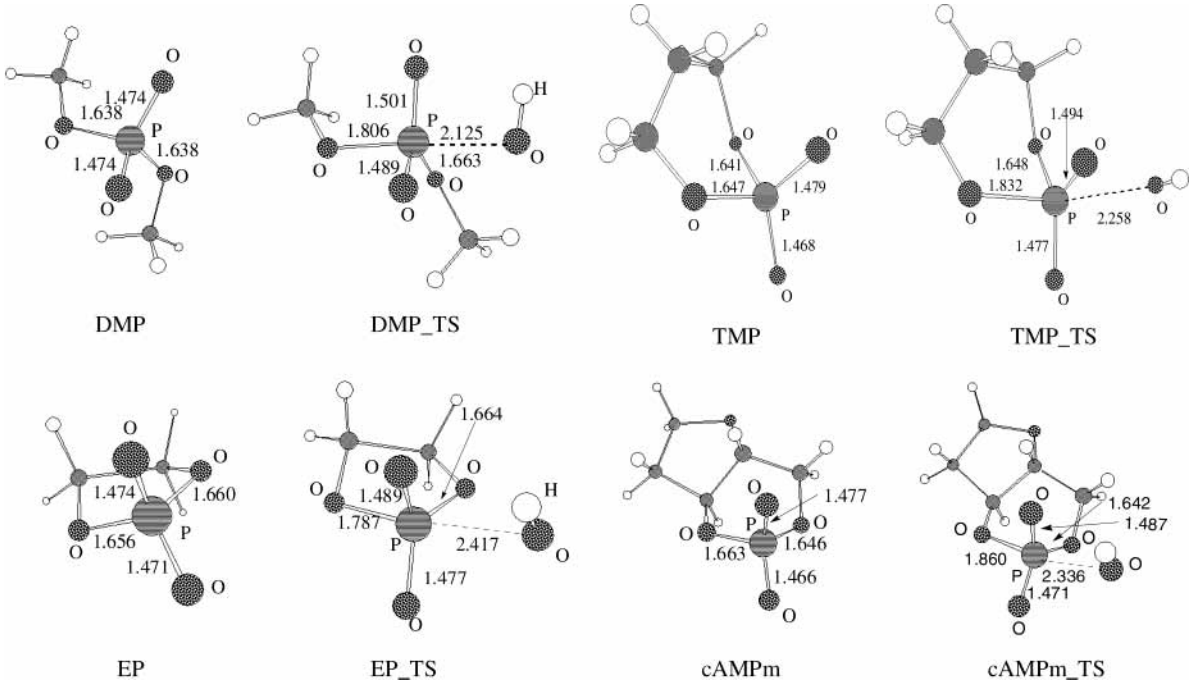

Figure 1. Geometries optimized at the HF/6-31+G* level for DMP, TMP, EP, and cAMPm and the corresponding transition states for the alkaline hydrolysis.

the structure featuring the attack of hydroxide ion at the P atom; the internuclear distances between the P atom and the hydroxide oxygen are all between 2.125 and 2.417 Å. Summarized in Table 1 are the activation free energies calculated with various SCRF procedures for the alkaline hydrolysis of four representative phosphodiesters in aqueous solution compared with those estimated from available experimental kinetic data. The activation free energy calculated for phosphodiester hydrolysis is the free energy change from the individual solvated reactants, $(RO)(R'O)P(O)O^- + OH^-$, to the corresponding transition state. As seen in Table 1, the activation free energy calculated in the gas phase for cAMPm hydrolysis at the MP2/6-31++G** level is lower than the corresponding value calculated at the MP2/6-31+G* level by only ~0.2 kcal/mol. This suggests that the 6-31+G* basis set used in our calculations is indeed sufficient for these reaction systems.

As seen from the activation free energies listed in Table 1, all of the SCRF calculations consistently predict that the solvent effects dramatically decrease the activation free energies for all of the phosphodiesters. The activation free energy for the reaction in the gas phase at $T = 298$ K and $P = 1$ atm is as high as ~89 kcal/mol for cAMPm and ~95 kcal/mol for DMP, TMP, and EP. The largest difference among the activation free energies calculated for DMP, TMP, and EP is smaller than 1 kcal/ mol as the sizes of these three phosphodiesters are very close to each other, whereas the activation free energy calculated for cAMPm, whose size is significantly larger, is ~6 kcal/mol lower than those for the other three smaller phosphodiesters. Our results calculated in the gas phase are very close to what is reported by Dejaegere and Karplus,[16] who did ab initio calculations on DMP and EP. Their best estimates of the activation free energies, 95.6 kcal/mol for DMP and 94.0 kcal/mol for EP, from a combination of the MP2/6-31+G* and HF/3−31+G-(d, d) calculations,[16] are close to our results. It appears that the activation free energies for the reactions in the gas phase are dependent on the size of the phosphodiester. This is likely because of some additional contribution to the stabilization of the highly charged transition state structure from the larger chemical environment of the reaction center of the ester hydrolysis. The larger the phosphodiester, the more diffused the additional negative charge provided by the hydroxide ion in the transition state structure, and the more stable the transition state structure. The similar argument may also stand for the solvent environmental effects that significantly stabilize the charged transition state structure for all of the four phosphodiesters.

We can compare our calculated energetic results with available experimental kinetic data for the reactions in aqueous solution. Numerous experimental kinetic data were reported on the hydrolysis of phosphodiesters.[3,4,19] Based on the experimental kinetic data, the activation free energy at 25 °C (i.e., $T = 298$ K) and $P = 1$ atm for the alkaline hydrolysis of the acyclic phosphodiester, DMP, in aqueous solution was estimated to be ~32 kcal/mol by Dejaegere and Karplus[16] based on the experimental second-order rate constant values (at 125 °C and 115 °C) determined by Westheimer et al.[3] We note that the activation free energy estimated from the second-order rate constant refers to the standard reactant state of 1 M for both DMP and HO^-. TMP (a phosphodiester with a six-membered ring) reacts at very nearly the same rate as an acyclic phosphodiester[19] and, therefore, should have a nearly the same activation free energy. The alkaline hydrolysis of EP (a phosphodiester with a five-membered ring) was found to be faster than that of DMP by about 10^6-10^8 times based on the available experimental rate constants.[19] Thus, the activation free energy for the EP hydrolysis should be lower than that for DMP by about 8 to 11 kcal/mol according to the conventional transition state theory.[42] As the activation free energy for the DMP hydrolysis was estimated to be ~32 kcal/mol, the activation free energy for the EP hydrolysis should be about 21 to 24 kcal/mol. For example, the experimental rate constant value[19] of 4.74×10^{-4} M^{-1} s^{-1} at 25 °C gives an activation free energy value of 22.0 kcal/mol according to the conventional transition state theory (CTST),[42] that is,

$$k = (k_B T/h)\exp(-\Delta G/k_B T) \quad (1)$$

where k_B is the Boltzmann constant, T is the absolute temper-

TABLE 1: Calculated Activation Free Energies (in kcal/mol) for the Reactions in the Gas Phase and in Aqueous Solution in Comparison with Available Experimental Data

	activation free energy			
calculation method[a]	DMP[d]	TMP[d]	EP[d]	cAMPm[d]
ΔG (gas)	95.3	95.4	94.5	89.0 (88.8)[i]
ΔG (SVPE, 0.002)$_{elec}$[b]	33.7	32.2	25.1	30.2
ΔG (SVPE, 0.001)$_{elec}$	33.1	32.0	25.1	29.6
ΔG (SPE, 0.002)$_{elec}$[b]	49.7	48.4	43.9	49.9
ΔG (SPE, 0.001)$_{elec}$	40.8	39.9	32.9	39.0
$\Delta G_{non-elec}$[c]	−0.5	−0.4	−0.3	−0.2
ΔG (SVPE, 0.002)$_{elec}$ + $\Delta G_{non-elec}$[b]	33.2	31.8	24.8	30.0
ΔG (SVPE, 0.001)$_{elec}$ + $\Delta G_{non-elec}$	32.6	31.6	24.8	29.4
ΔG (PCM)	43.1	50.0	42.8	49.4
ΔG (COSMO)	46.9	52.5	44.5	51.8
ΔG (IEFPCM)	42.3	48.2	40.3	47.2
Dejaegere and Karplus[e]	37.7		29.6	
expt	∼32[f]	∼32[g]	∼21−24[h]	∼29[j]

[a] ΔG (gas) are the activation free energies in the gas phase (T = 298 K and P = 1 atm) determined at the MP2/6-31+G(d) level by using the geometries optimized at the HF/6-31+G(d) level. The activation free energies calculated in aqueous solution are sums of ΔG (gas) and the corresponding solvent shifts determined by the SCRF calculations at the HF/6-31+G(d) level. The SCRF calculations were performed by using the geometries optimized at the HF/6-31+G(d) level in gas phase. [b] 0.002 au, instead of 0.001 au, contour value was used in the SCRF calculations. [c] The total contribution of nonelectrostatic interactions to the activation free energy determined by the PCM calculations. The corresponding IEFPCM and COSMO calculations led to exactly the same values. [d] The phosphodiesters are dimethyl phosphate (DMP), trimethylene phosphate (TMP), ethylene phosphate (EP), and a ribose-like model (cAMPm) of cAMP. [e] The results calculated by Dejaegere and Karplus[16] at the MP2 level in the gas-phase plus the solvent shifts calculated with a continuum solvation model using the van der Waals envelope and partial atomic charges determined at the HF/6-31G*//HF/ 3-21+G(d,d) level. [f] Experimental estimate from Dejaegere and Karplus.[16] [g] Experimental estimate based on the observation that the alkaline hydrolysis rate of TMP is nearly the same as that of DMP.[19] [h] Experimental estimate based on the observation that the alkaline hydrolysis of EP is about $10^6 - 10^8$ times faster than that of DMP.[19] [i] Value in the bracket is the activation free energy calculated at the MP2/6-31++G(d, p) level in the gas phase. [j] Experimental estimate based on the first-order rate constant reported by Chin and Zou.[43]

ature, h is Planck's constant, and ΔG is the activation free energy. The other rate constant values collected in Table 9 of the reference[19] lead to different activation free energy values. In addition, the experimental first-order rate constant for the alkaline hydrolysis of cAMP was also estimated to be 3.0×10^{-14} s^{-1} at 50 °C in neutral water (i.e., pH 7) by Chin and Zou.[43] This first-order rate constant value suggests that the corresponding second-order rate constant should be 3.0×10^{-7} M^{-1} s^{-1} at 50 °C.

As seen in Table 1, the activation free energies calculated by using the SVPE method with the 0.002 au contour are very close to the corresponding values calculated with the default 0.001 au contour; the largest difference is only 0.6 kcal/mol. The results of the SVPE calculations, which accurately evaluate volume polarization, are rather insensitive to the used contour value that determines the solute cavity size. Further including contributions from the short-range nonelectrostatic interactions, the calculated free energy energies all slightly decrease; the largest change is 0.5 kcal/mol in magnitude. The small contributions from the short-range nonelectrostatic interactions are consistent with our earlier finding in a computational study on the alkaline hydrolysis of carboxylic acid esters,[39] which further confirms that the overall effects of the short-range nonelectrostatic interactions on the activation free energies of chemical reactions are nearly canceled out. As seen in Table 1, the activation free energies determined by the SVPE calculations using the 0.001 and 0.002 au contours are all in good agreement with available experimental data. The SVPE results discussed below will refer to those calculated with the default 0.001 au contour plus the corrections of short-range nonelectrostatic interactions.

According to the SVPE calculations, the activation free energy, 32.6 kcal/mol, calculated for the DMP hydrolysis is in excellent agreement with the experimental estimate, ∼32 kcal/mol. The activation free energies 31.6 and 29.4 kcal/mol calculated for the hydrolysis of TMP and cAMPm, respectively, are also in excellent agreement with the experimental estimates, ∼32 kcal/mol for the TMP hydrolysis and ∼29 kcal/mol for the cAMP hydrolysis. The activation free energy, 24.8 kcal/mol, calculated for the EP hydrolysis is also in good agreement with the experimental estimate, ∼ 21−24 kcal/mol. The calculated shift of the activation free energy from DMP to EP is ∼8 kcal/mol, which is in good agreement with the experimental shift, ∼ 8−11 kcal/mol. Our calculated results clearly show that the larger change of activation free energy, and the corresponding considerable change of the alkaline hydrolysis rate, from DMP to EP is indeed mainly attributed to the difference in the solvent shift between the two reactions. The solvation more favorably stabilizes the transition state structure of the EP hydrolysis in comparison with the DMP hydrolysis. Our results strongly support the qualitative conclusion of Dejaegere and Karplus,[16] whose ab initio calculations led to the activation free energies 37.7 kcal/mol for the DMP hydrolysis and 29.6 kcal/mol for the EP hydrolysis, that the remarkable difference in the hydrolysis rate between DMP and EP is mainly due to the solvation rather than the ring-strain. Quantitatively, the calculations reported by Dejaegere and Karplus[16] systematically overestimated the activation free energies by ∼6 kcal/mol, whereas our SVPE results are much closer to the experimental data as seen in Table 1.

Comparing the results determined by the SPE calculations neglecting volume polarization with the corresponding SVPE results, it can be found that the volume polarization effect changes the activating free energies for the considered reaction systems by 7.7−9.4 kcal/mol when the 0.001 au contour is used and by 16.0−19.7 kcal/mol when the 0.002 au contour is used. Neglecting volume polarization, the calculated results become very sensitive to the used contour value that determines the solute cavity. The differences between the SVPE and SPE results for the hydrolysis of phosphodiesters are larger than those obtained in our previous study on alkaline hydrolysis of carboxylic acid esters.[39] This is because the volume polarization effect is more important for a system that has more solute charge penetrating outside the solute cavity. The reaction systems considered in this study are all doubly negatively charged, whereas the previously considered reaction systems are all singly negatively charged. Nevertheless, compared to the SVPE results and experimental data, the SPE calculations only systematically overestimated the activation free energies. The relative values of the calculated activation free energies are still in good agreement with the SVPE results and available experimental data.

We also considered the results calculated with other three SCRF methods, that is, PCM, IEFPCM, and COSMO. As seen in Table 1, within these three SCRF methods, the activation free energies calculated by using the COSMO method are generally larger than those calculated by using the other two SCRF methods. IEFPCM is an improved version of PCM. The

activation free energies determined by IEFPCM are slightly closer to the experimental activation free energies than those determined by PCM or COSMO. However, all of these three SCRF methods significantly overestimated the activation free energies. The relative values of the calculated activation free energies are also significantly different from the relative values of the SVPE results and available experimental data. According to both the SVPE results and experimental data, the activation free energy for the TMP hydrolysis should be very close to that for the DMP hydrolysis, whereas the activation free energy for the EP hydrolysis should be about 8−11 kcal/mol lower than that for the DMP hydrolysis. However, according to the PCM, IEFPCM, and COSMO calculations, the activation free energy for the TMP hydrolysis is significantly higher than that for the DMP hydrolysis (by 5.6−6.9 kcal/mol), whereas the activation free energy for the EP hydrolysis is only 0.3−2.4 kcal/mol lower than that for the DMP hydrolysis.

Conclusion

We performed a series of first-principles electronic structure calculations to study alkaline hydrolysis of four representative phosphodiesters, that is, dimethyl phosphate (DMP), trimethylene phosphate (TMP), ethylene phosphate (EP), and a simplified model (cAMPm) of adenosine 3′, 5′-phosphate (cAMP). Reaction coordinate calculations show that for all of these phosphodiesters the alkaline hydrolysis follows a one-step bimolecular mechanism initialized by the attack of an hydroxide ion at the phosphorus atom of the ester. Five SCRF methods, that is, SVPE, SPE, PCM, IEFPCM, and COSMO, were used to calculate the activation free energies and the calculated results were compared with the available experimental data. It has been shown that the SVPE calculations, which accurately evaluate volume polarization, are rather insensitive to the used solute charge isodensity contour value that determines the solute cavity size. The activation free energies (32.6, 31.6, 24.8, and 29.4 kcal/mol for DMP, TMP, EP, and cAMPm, respectively) calculated by the SVPE method with the corrections of nonelectrostatic interactions are all in good agreement with the available experimental data (∼32, ∼32, ∼21−24, and ∼29 kcal/mol for DMP, TMP, EP, and cAMP, respectively). The SVPE results show that the solvent effects dramatically decrease the activation free energies for the alkaline hydrolysis of phosphodiesters and strongly support the conclusion that the remarkable difference in the hydrolysis rate between DMP and EP is mainly due to the solvation, rather than the ring-strain. Compared to the SVPE results and available experimental data, the SPE calculations neglecting volume polarization systematically overestimated the activation free energies, but the relative values of the SPE results are also in qualitative agreement with those of the SVPE results and available experimental data. The PCM, IEFPCM, and COSMO calculations also overestimated the activation free energies and the relative values of these results are all significantly different from those of the SVPE results and available experimental data.

Supporting Information Available: Absolute energies calculated in the gas phase and solvent shifts calculated with various SCRF methods by using the geometries optimized at the HF/6-31+G(d) level in the gas phase. This material is available free of charge via the Internet at http://pubs.acs.org.

References and Notes

(1) Westheimer, F. H. *Science* **1987**, *235*, 1173.
(2) Callahan, S. M.; Cornell, N. W.; Dunlap, P. V. *J. Biol. Chem.* **1995**, *270*, 17627.
(3) (a) Kumamoto, J.; Cox, J. R.; Westheimer. F. H. *J. Am. Chem. Soc.* **1956**, *78*, 4858. (b) Haake, P. C.; Westheimer, F. H. *J. Am. Chem. Soc.* **1961**, *83*, 1102.
(4) (a) Westheimer, F. H. *Chem. Rev.* **1981**, *4*, 313. (b) Hengge, A. C.; Cleland, W. W. *J. Am. Chem. Soc.* **1990**, *112*, 7421.
(5) Admiraal, S. J.; Herschlag, D. *Chem. Biol.* **1995**, *2*, 729.
(6) Maegley, K. A.; Admiraal, S. J.; Herschlag, D. *Proc. Natl. Acad. Sci. U.S.A.* **1996**, *93*, 8160.
(7) Florian, J.; Warshel, A. *J. Am. Chem. Soc.* **1997**, *119*, 5473.
(8) Aqvist, J.; Kolmodin, K.; Florian, J.; Warshel, A. *Chem. Biol.* **1999**, *6*, R71.
(9) Zheng, F.; Zhan, C.-G.; Ornstein, R. L. *J. Chem. Soc., Perkin Trans. 2* **2001**, 2355.
(10) Lim, C.; Karplus, M. *J. Am. Chem. Soc.* **1990**, *112*, 5872.
(11) Dejaegere, A.; Lim, C.; Karplus, M. *J. Am. Chem. Soc.* **1991**, *113*, 4353.
(12) Lim, C.; Tole, P. *J. Phys. Chem.* **1992**, *96*, 5217.
(13) Tole, P.; Lim, C. *J. Phys. Chem.* **1993**, *97*, 6212.
(14) Tole, P.; Lim, C. *J. Am. Chem. Soc.* **1994**, *116*, 3922.
(15) Chang, N.-Y.; Lim, C. *J. Am. Chem. Soc.* **1998**, *120*, 2167.
(16) Dejaegere, A.; Karplus, M. *J. Am. Chem. Soc.* **1993**, *115*, 5316.
(17) Dejaegere, A.; Liang, X. L.; Karplus, M. *J. Chem. Soc., Faraday Trans.* **1994**, *90*, 1763.
(18) Lopez, X.; Dejaegere, A.; Karplus, M. *J. Am. Chem. Soc.* **2001**, *123*, 11755.
(19) Cox, J. R., Jr.; Ramsay, O. B. *Chem. Rev.* **1964**, *64*, 317.
(20) Dudev, T.; Lim, C. *J. Am. Chem. Soc.* **1980**, *102*, 4450.
(21) Jenkins, L. A.; Bashkin, J. K.; Pennock, J. D.; Florian, J.; Warshel, A. *Inorg. Chem.* **1999**, *38*, 3215.
(22) Lopez, X.; Schaefer, M.; Dejaegere, A.; Karplus, M. *J. Am. Chem. Soc.* **2002**, *124*, 5010.
(23) Lopez, X.; York, D. M.; Dejaegere, A.; Karplus, M. *J. Comput. Chem.* **2002**, *86*, 20.
(24) Florian, J.; Goodman, M. F.; Warshel, A. *J. Am. Chem. Soc.* **2003**, *125*, 8163.
(25) Chen, X.; Zhan, C.-G. *J. Phys. Chem. A* **2004**, *108*, 3789.
(26) Hehre, W. J.; Radom, L.; Schleyer, P. v. R.; Pople, J. A. *Ab Initio Molecular Orbital Theory*; John Wiley & Sons: New York, 1986.
(27) (a) Gonzalez, C.; Schlegel, H. B. *J. Chem. Phys.* **1989**, *90*, 2154. (b) Gonzalez, C.; Schlegel, H. B. *J. Phys. Chem.* **1990**, *94*, 5523.
(28) Zhan, C.-G.; Landry, D. W.; Ornstein, R. L. *J. Am. Chem. Soc.* **2000**, *122*, 1522.
(29) Zhan, C.-G.; Landry, D. W.; Ornstein, R. L. *J. Am. Chem. Soc.* **2000**, *122*, 2621.
(30) Florian, J.; Warshel, A. *J. Phys. Chem. B* **1998**, *102*, 719.
(31) (a) Miertus, S.; Scrocco, E.; Tomasi, *J. Chem. Phys.* **1981**, *55*, 117. (b) Miertus, S.; Tomasi. J. *Chem. Phys.* **1982**, *65*, 239. (c) Cossi, M.; Barone, V.; Cammi, R.; Tomasi, J. *Chem. Phys. Lett.* **1996**, *255*, 327.
(32) (a) Cances, M. T.; Mennucci, B.; Tomasi, J. *J. Chem. Phys.* **1997**, *107*, 3032. (b) Cossi, M.; Barone, V.; Mennucci, B.; Tomasi, J. *Chem. Phys. Lett.* **1998**, *286*, 253. (c) Mennucci, B.; Cammi, R.; Tomasi, J. *J. Chem. Phys.* **1998**, *109*, 2798.
(33) Barone, V.; Cossi, M. *J. Phys. Chem. A* **1998**, *102*, 1995.
(34) Frisch, M. J.; Trucks, G. W.; Schlegel, H. B.; Scuseria, G. E.; Robb, M. A.; Cheeseman, J. R.; Zakrzewski, V. G.; Montgomery, J. A.; Stratmann, R. E.; Burant, J. C.; Dapprich, S.; Millam, J. M.; Daniels, A. D.; Kudin, K. N.; Strain, M. C.; Farkas, O.; Tomasi, J.; Barone, V.; Cossi, M.; Cammi, R.; Mennucci, B.; Pomelli, C.; Adamo, C.; Clifford, S.; Ochterski, J.; Petersson, G. A.; Ayala, P. Y.; Cui, Q.; Morokuma, K.; Malick, D. K.; Rabuck, A. D.; Raghavachari, K.; Foresman, J. B.; Cioslowski, J.; Ortiz, J. V.; Stefanov, B. B.; Liu, G.; Liashenko, A.; Piskorz, P.; Komaromi, I.; Gomperts, R.; Martin, R. L.; Fox, D. J.; Keith, T.; Al-Laham, M. A.; Peng, C. Y.; Nanayakkara, A.; Gonzalez, C.; Challacombe, M.; Gill, P. M. W.; Johnson, B.; Chen, W.; Wong, M. W.; Andres, J. L.; Gonzalez, A. C.; Head-Gordon, M.; Replogle, E. S.; Pople, J. A. *Gaussian 98*, Revision A.7; Gaussian, Inc.: Pittsburgh, PA, 1998
(35) (a) Tomasi, J.; Persico, M. *Chem. Rev.* **1994**, *94*, 2027. (b) Cramer, C. J.; Truhlar, D. G. In *Solvent Effects and Chemical Reactions*; Tapia, O., Bertran, J., Eds.; Kluwer: Dordrecht, The Netherlands, 1996; p 1. (c) Cramer, C. J.; Truhlar, D. G. *Chem. Rev.* **1999**, *99*, 2161. (d) Chipman, D. M. *J. Chem. Phys.* **1997**, *106*, 10194. (e) Chipman, D. M. *J. Chem. Phys.* **1999**, *110*, 8012. (f) Chipman, D. M. *J. Chem. Phys.* **2000**, *112*, 5558.
(36) Zhan, C.-G.; Bentley, J.; Chipman, D. M. *J. Chem. Phys.* **1998**, *108*, 177.
(37) Zhan, C.-G.; Chipman, D. M. *J. Chem. Phys.* **1998**, *109*, 10543.
(38) Zhan, C.-G.; Chipman, D. M. *J. Chem. Phys.* **1999**, *110*, 1611.
(39) Zhan, C.-G.; Landry, D. W.; Ornstein, R. L. *J. Phys. Chem. A* **2000**, *104*, 7672.
(40) (a) Zhan, C.-G.; Niu, S.; Ornstein, R. L. *J. Chem. Soc., Perkin Trans. 2* **2001**, *1*, 23. (b) Zhan, C.-G.; Dixon, D. A. *J. Phys. Chem. A* **2001**, *105*, 11534. (c) Dixon, D. A.; Feller, D.; Zhan, C.-G.; Francisco, J. S. *J. Phys. Chem. A* **2002**, *106*, 3191. (d) Zheng, F.; Zhan, C.-G.; Ornstein, R.

L. *J. Phys. Chem. B* **2002**, *106*, 717. (e) Zhan, C.-G.; Dixon, D. A. *J. Phys. Chem. A* **2002**, *106*, 9737. (f) Zhan, C.-G.; Dixon, D. A.; Sabri, M. I.; Kim, M.-S.; Spencer, P. S. *J. Am. Chem. Soc*. **2002**, *124*, 2744. (g) Zhan, C.-G.; Dixon, D. A. *J. Phys. Chem. A* **2003**, *107*, 4403. (h) Zhan, C.-G.; Dixon, D. A.; Spencer, P. S. *J. Phys. Chem. B* **2003**, *107*, 2853. (i) Dixon, D. A.; Feller, D.; Zhan, C.-G.; Francisco, S. F. *Int. J. Mass Spectrom*. **2003**, *227*, 421.

(41) Schmidt, M. W.; Baldridge, K. K.; Boatz, J. A.; Elbert, S. T.; Gordon, M. S.; Jensen, J. H.; Koseki, S.; Matsunaga, N.; Nguyen, K. A.; Su, S. J.; Windus, T. L.; Dupuis, M.; Montgomery, J. A. *J. Comput. Chem.* **1993**, *14*, 1347.

(42) Alvarez-Idaboy, J. R.; Galano, A.; Bravo-Pérez, G.; Ruíz, M. E. *J. Am. Chem. Soc.* 2001, 123, 8387.

(43) Chin, J.; Zou, X. *Can. J. Chem*. **1987**, *65*, 1882.